

Review

## High Electroactive Electrode Catalysts and Highly sensitive Electro analytical Techniques for Hydrogen Peroxide detection

Rasu Ramachandran<sup>1</sup>, Shen-Ming Chen<sup>2,\*</sup>, George peter Gnana kumar<sup>3</sup>, Pandi Gajendran<sup>1</sup>, Arulanandam Xavier<sup>1</sup>, Natrajan Biruntha Devi<sup>4</sup>

<sup>1</sup>Department of Chemistry, The Madura College, Vidya Nagar, Madurai – 625 011, Tamil Nadu, India.

<sup>2</sup>Electroanalysis and Bioelectrochemistry Lab, Department of Chemical Engineering and Biotechnology, National Taipei University of Technology, No.1, Section 3, Chung-Hsiao East Road, Taipei 106.Taiwan (ROC).

<sup>3</sup>Department of Physical Chemistry, School of Chemistry, Madurai Kamaraj University, Madurai-625 021, Tamil Nadu, India.

<sup>4</sup>Department of Chemistry, S.Vellaichamy Nadar College, Nagamalai pudukkottai, Madurai – 625021, Tamil Nadu, India.

\*E-mail: [smchen78@ms15.hinet.net](mailto:smchen78@ms15.hinet.net)

Received: 5 November 2015 / Accepted: 12 December 2015 / Published: 1 January 2016

---

This review article presents different orientation of electrochemical non-enzymatic biosensor hydrogen peroxide (H<sub>2</sub>O<sub>2</sub>) applications. Due to fabricate and immobilized novel based electrode materials have been used for the estimation of H<sub>2</sub>O<sub>2</sub> sensor. Most importantly for the development of this kind of sensor, this can be used in various fields, such as clinical, biology, chemistry, food production and clinical etc. The biosensor electrode catalysts were optimized with high sensitive (Chronoamperometry, differential pulse voltammetry and square wave voltammetry) electroanalytical techniques for H<sub>2</sub>O<sub>2</sub> detection. Finally, we have addressed, the biosensor parameters also promote their limit of detection (LOD) values, high selectivity, high sensitivity, good stability and future prospects in biosensor applications.

---

**Keywords:** Electrode catalyst, Hydrogen peroxide, Morphological effects, Biosensors, Cyclic stability.

### 1. INTRODUCTION

The use of high surface area and good biocompatibility electrode materials provides suitable nanomaterials in electro analysis and biosensor applications. An important milestone in the preparation of Horseradish peroxidase (HRP) enzyme immobilized on Sonogel-carbon electrode composite for the

usage of third generation hydrogen peroxide ( $\text{H}_2\text{O}_2$ ) biosensor [1]. This kind of  $\text{H}_2\text{O}_2$  biosensor, which can be applied in various fields, such as chemical industry, sterilization, food production and clinical applications *etc.* Salimi *et al* [2] used a single-walled carbon nanotube (SWCNT) based manganese complex composite electrode widely applied in non-enzymatic biosensor. To explain, a rapid and low-cost, novel biosensor of  $\text{Fe}_3\text{O}_4$ -Au magnetite nanoparticles were deposited on HRP and graphene sheets have been found to play an important role in the optimized detection of  $\text{H}_2\text{O}_2$  ( $1.2 \times 10^{-5}$  M) [3]. One of the most recognized metal oxide (Ag- $\text{MnO}_2$ -MWCNTs) nanocomposites can be used due to its long-term stability and high sensitivity with non-enzymatic sensor [4]. Li *et al* [5] constructed a new type of Au@ $\text{AuS}_2\text{O}_3$  core-shell nanomaterials and Chitosan-MWCNTs act as a composite membrane could be used in intrinsic electrocatalytic activity towards  $\text{H}_2\text{O}_2$  sensor. A simple temperature controlled poly(diallylmethylammonium chloride) (PDDA) which can be modified with self-assembled Prussian blue (PB) nanocube electrode offer great advantage in good sensitive amperometric biosensor [6]. Hybrid conducting three-dimensional graphene, carbon nanotube and  $\text{MnO}_2$  ( $\text{MnO}_2$ /graphene/CNTs) electrode catalysts have been developed with the hope of improving their proposed biosensor applications. Such composite may lead to the development of non-enzymatic biosensor estimation [7]. The electrode modification and electrochemical enhancement of surfactant/salt modifications based higher grade metallic substrate (Au, Pt and Ag) electrodes have been reported. The above prepared electro active metallic surface based electrode has been explored extensively for biosensor applications [8]. As a novel preparation of graphene/nafion/Azure I/Au nanoparticles composite has been fabricated, which it could be obtained the highly expected cheap electrode catalyst for the development of electrochemical behaviour properties of  $\text{H}_2\text{O}_2$  [9]. Molecular self-assembled alternating-charge protein method has been recognized as a new, efficient and versatile technique for the fabrication of partially quantized poly(4-vinyl pyridine) (QPVP). This electrode was generated by an excellent electrocatalytic effect on  $\text{H}_2\text{O}_2$  reduction [10]. Sheng *et al* [11] suggested sol-gel technique for the preparation of pyrocatechol violet (PCV) modified carbon ceramic electrode (CCE) and was resulted the modified electrode exhibited a well-defined redox couple due to the oxidation and reduction of quinone-hydroquinone. The exhibited electrocatalytic activities towards  $\text{H}_2\text{O}_2$  (Sensitivity =  $11.2 \text{ nA } \mu\text{M}^{-1}$  and LOD =  $4 \times 10^{-6}$  M). In a pioneering work, ZnO- $\text{SnO}_2$  nanotube composite was prepared by electro spinning method. The prepared ZnO- $\text{SnO}_2$  composite resulted great potential application in semiconductor and in photo electrochemical (PEC) performance in  $\text{H}_2\text{O}_2$  detection [12]. The electrochemical strategy was adopted to prepare the functionalized Au electrode with the electropolymerization of 2-mercaptoethane sulfonic acid, 3-mercaptophenylboronic acid and *p*-aminothiophenol. While the electropolymerized electrode ensured the use for the construction of a reagentless biosensor for  $\text{H}_2\text{O}_2$  [13]. The bimetallic nature of Ag seeds based Cu (Ag@Cu) nanowire modified electrode has been used as a transducer in enhancing electrocatalytic ( $3 \times 10^{-6}$  M) activity in unzipped amperometric  $\text{H}_2\text{O}_2$  sensor [14]. Recently, different electrode materials (Carbon, carbon nanotubes, metal oxides, conducting polymers and nanocomposites) were widely used in various electrochemical applications such as supercapacitors [15], solar cells [16], sensors [17], pesticide sensors [18], biosensors [19, 20], fuel cells [21] and microbial fuel cell [22] *etc.*

In the present work discussed with the recent development electrode fabrication methods and various types of morphological electrode materials in non-enzymatic  $\text{H}_2\text{O}_2$  sensor applications. In particular, this article is mainly focused in different morphological effects, optimum pH and various electrochemical sensitive techniques for the determination of biosensor studies.

## 2. ELECTRODE CATALYSTS

### 2.1. Carbon

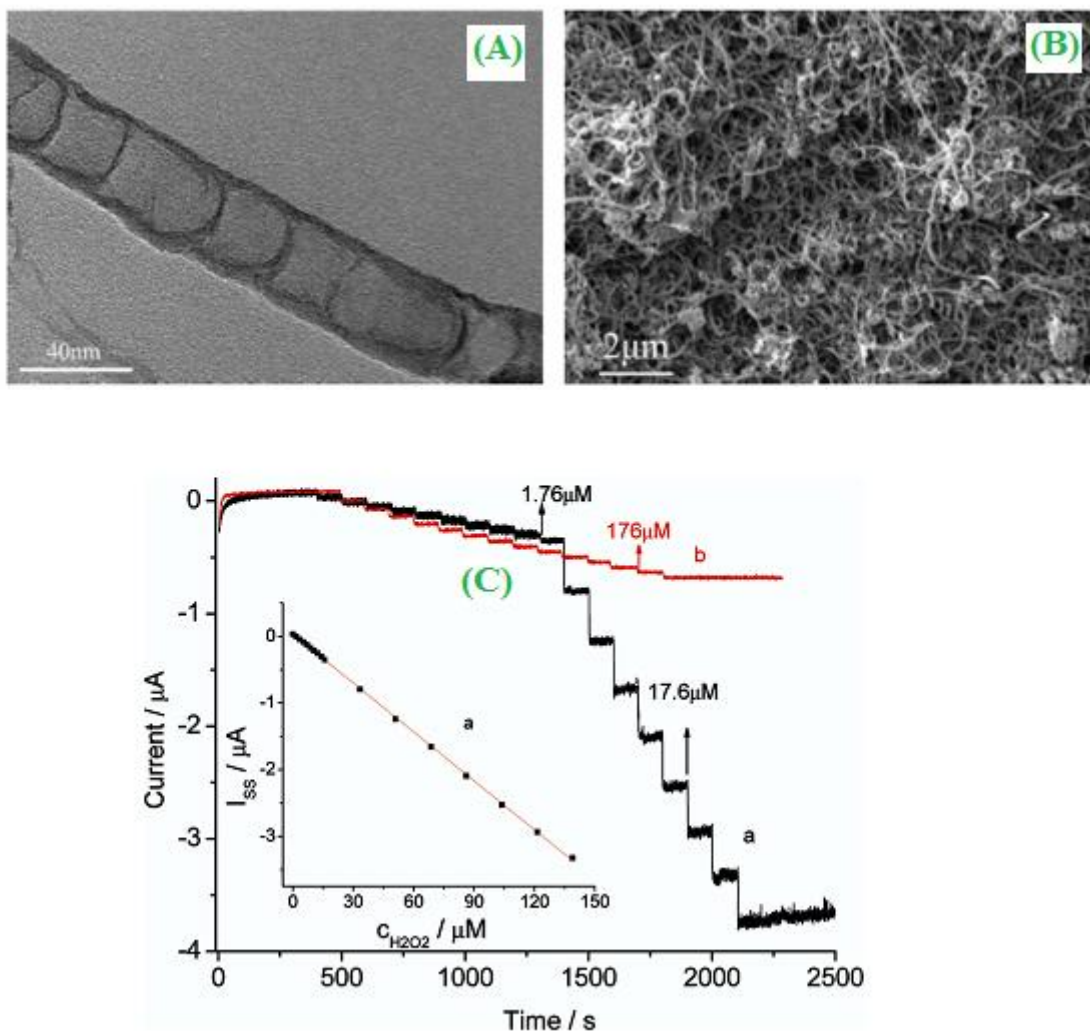


**Figure 1.** (A) TEM and (B) SEM images of NCNTs. (C) Current-time curve of (a) NCNT/GC and (b) MWCNT/GC electrodes with successive addition of  $\text{H}_2\text{O}_2$  (indicated by arrows for marked concentrations) in 0.10 M, pH 7.4, PBS at an applied potential of +0.3 V vs SCE). ("Reprinted with permission from (*ACS Nano* 4 (2010) 4292-4298). Copyright (2010) American Chemical Society").

Most of the biosensors have been using carbon based electrode materials; it has novel optical, electronic, mechanical and catalytic properties etc. A novel double stranded *dsDNA*, which can be

wrapped with single-walled carbon nanotube (SWCNT) by using an aqueous solution. The modified (*dsDNA*-SWCNT) hybrids were used to detect  $\text{H}_2\text{O}_2$  and glucose [23]. A systematic two step (Chemical vapour deposition and one-step reduction) processes have been used for the fabrication of palladium supported helical carbon nanofiber hybrid (Nafion/Pd-HCNFs/GCE). The modified electrode was immobilized with glucose oxidase ( $\text{GO}_x$ ) and the resulted sensing response of glucose with a wide range (0.06 - 6.0 mM) and their limit of detection (LOD) value of 0.03 mM [24]. Most notable, chemical vapour deposition (CVD) method has been used for the synthesis of nitrogen-doped carbon nanotubes (NCNTs). The as-synthesized bamboo-shaped structure of NCNTs diameter around 30-35 nm (Fig.1A) and a three-dimensional homogeneous membrane of NCNTs as shown in Fig.1B. The displayed current-time curve of NCNTs/GCE, the linear response sensor of  $\text{H}_2\text{O}_2$  from 1.76 to 1.9  $\mu\text{M}$  and their estimated LOD value of  $0.37 \times 10^{-6}$  M (Fig.1C) [25]. The use of commercially received low-cost hemoglobin modified impure-multi-walled carbon nanotube (GCE/i-MWCNT@Hb/N<sub>F</sub>) electrode catalyst for efficient direct electron transfer studies. A coil-like structure exhibits uniform and smooth surface, the electrode catalysts were used amperometry technique for highly selective and sensing of  $\text{H}_2\text{O}_2$  (300  $\mu\text{M}$ ) [26]. For the development of three different inorganic/organic doped carbon aerogel (CA) electrode materials (Ni-CA, Pd-CA and PPy-CA) were mixed with ionic liquid (IL) to form three stable composite electrodes. These three hybrid electrodes were significantly bioelectrocatalytically improve the  $\text{H}_2\text{O}_2$  detection limit values of 1.68, 1.02 and  $0.85 \times 10^{-6}$  M, respectively [27]. HiPco based carbon nanotube has received much attention for the interest in enzyme-catalyzed *in vitro* and *in vivo*  $\text{H}_2\text{O}_2$  sensor; the demonstrated electrode catalyst optically detects the glucose molecules [28]. Chemical synthesis has become a popular method to prepare a three-dimensional (Polybenzimidazole and carboxylated multi-walled carbon nanotube) (PBI-MWCNT-COOH) composite, then it was further modified with gold electrode for the detection of  $\text{H}_2\text{O}_2$ , the amperometric linear concentration range from  $6.25 \times 10^{-6}$  M to  $10 \times 10^{-3}$  M [29].

## 2.2. Metal oxides

One of the most exciting facile rout synthesis of porous  $\text{Co}_3\text{O}_4$  nano wire arrays. By using scanning electron microscope (SEM) technique, the thin film electrode surface area, diameter around 500 nm and their length up to 15  $\mu\text{M}$ . The free standing of meso porous quasi-single crystalline  $\text{Co}_3\text{O}_4$  nano wire, which can be used for sensing of  $\text{H}_2\text{O}_2$ . The optimized linear curve  $\text{H}_2\text{O}_2$  concentration region from 5 to 30 mM [30]. A non-enzyme based  $\text{H}_2\text{O}_2$  sensor has been optimized by nickel oxide (NiO) supported graphene nanosheet. The template synthesized nickel based electrode attracted much attention due to its lowest detection limit ( $0.4 \times 10^{-6}$  M) and high sensitivity ( $1077 \text{ mA mM}^{-1} \text{ cm}^{-2}$ ) [31]. A simple and sensitive amperometric determination of  $\text{H}_2\text{O}_2$  has been estimated by using ruthenium oxide modified riboflavin (GC/RuO<sub>x</sub>/RF) nanocomposite. The novel electrocatalytic activity towards the  $\text{H}_2\text{O}_2$  reduction and the estimated catalytic rate constant ( $K_{cat}$ ) value of  $9.1 \times 10^3 \text{ M}^{-1} \text{ s}^{-1}$  [32]. Butwong *et al* [33] have been electrochemically deposited of cadmium oxide (CdO) on glassy carbon electrode (GCE) and then further modified with MWCNT electrode. The modified metal oxide (CdO/MWCNT) composite for sensor studies have been developed with the hope of improving the

possibility and finding of  $\text{H}_2\text{O}_2$  detection limit value of  $0.1 \times 10^{-6}$  M. An efficient and microwave-assisted synthesis of platinum supported manganese oxide ( $\text{Pt-MnO}_x$ ) electrode may lead to the development of a novel electrochemical  $\text{H}_2\text{O}_2$  sensors in which indicated the oxidation current of  $\text{H}_2\text{O}_2$  was linear and the LOD value of  $0.7 \times 10^{-6}$  M [34]. Autoclave (Heated at  $180^\circ\text{C}$  for 18h) method has been extensively used for the preparation of hierarchical hollow spheres like  $\text{MnO}_3$  electrode. The uniform hollow spheres nanoparticles ( $\sim 20$  nm diameter) have been evaluated for which sensitive and selective non-enzymatic electrochemical sensor studies [35]. There has been a three-step explosive preparation of iron oxide based polypyrrole nanocomposite on silver nanoparticle ( $\text{Fe}_3\text{O}_3/\text{PPy}/\text{Ag}$ ) for non-enzymatic  $\text{H}_2\text{O}_2$  [36].

### 2.3. Conducting polymers

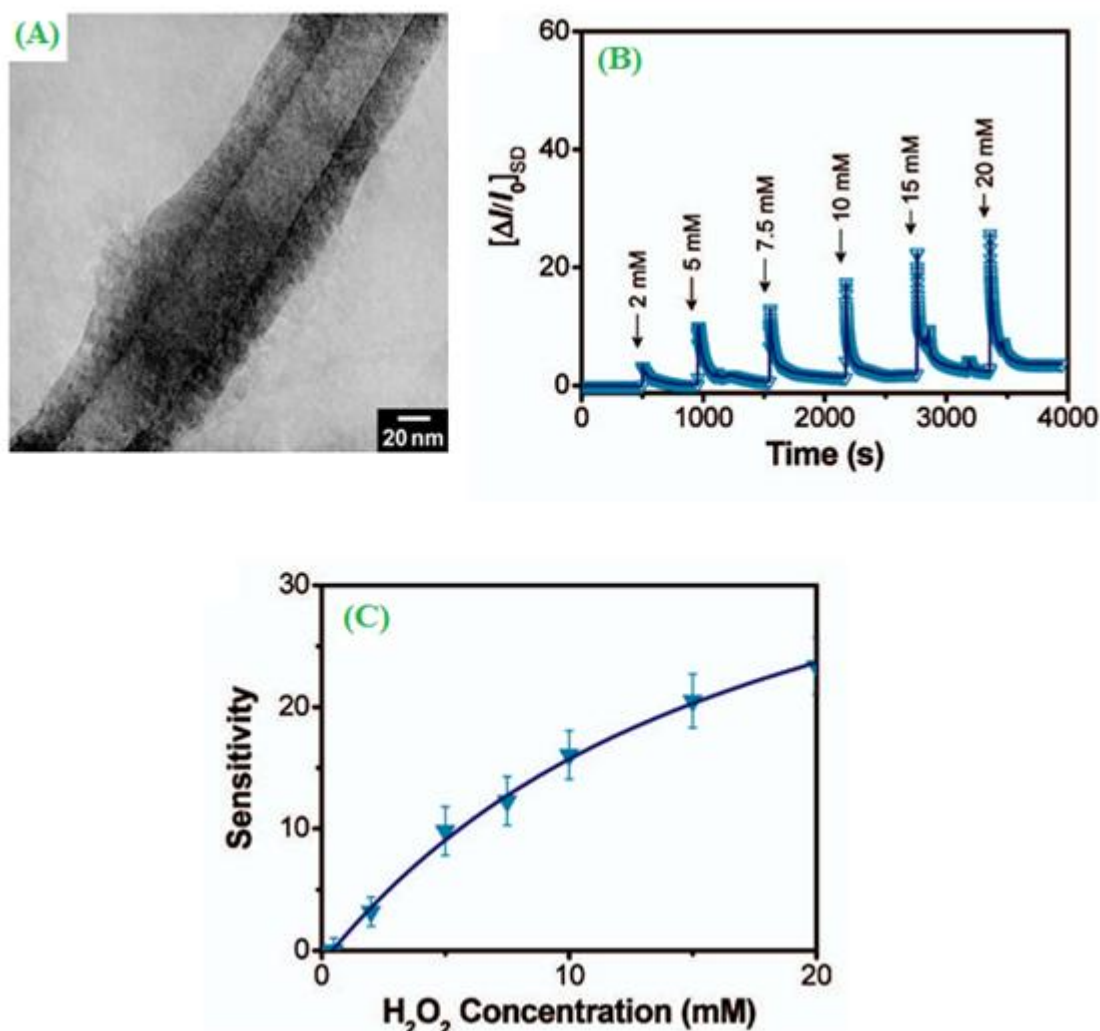


**Figure 2.** Typical TEM image of CPNTs (A) after  $\text{GO}_x$  immobilization. Response of a  $\text{GO}_x$ -CPNT FET sensor to  $\text{H}_2\text{O}_2$  at VSD)  $-10$  mV: (B) real-time ISD change upon consecutive addition of 2-20 mM  $\text{H}_2\text{O}_2$ ; (C) calibration curve of sensitivity versus  $\text{H}_2\text{O}_2$  concentration. ("Reprinted with permission from (*J. Phys. Chem. B* 112 (2008) 9992-9997). Copyright (2008) American Chemical Society").

Enzyme based functionalized carboxylated polypyrrole nanotubes (CPNTs) have been prepared by vapour deposition.

Fig.2A. Showed TEM image of after the  $\text{GO}_x$  immobilization of CPNTs, the potential array of field-effect transistor (FET) sensor, which can detect the various  $\text{H}_2\text{O}_2$  concentration levels (Fig.2(B&C)) [37]. The attractiveness conductivity of N-alkylated polyaniline, which can exciting apply for the detection of  $\text{H}_2\text{O}_2$  and their suggested sensitive lowest detection value of  $<1$  ppm level at neutral conditions [38]. Platinum coated poly(Allylamine)/poly(vinylsulfate) polyelectrolyte multilayer (PEM) film has become an important class of electrode materials for the simultaneous determination of  $\text{H}_2\text{O}_2$ , ascorbic acid (AA), uric acid (UA) and acetaminophenone [39]. Conducting polymer of polyaniline modified poly(acrylic acid) nanojunction electrodes are expected to be a very promising for application in non-enzyme based  $\text{H}_2\text{O}_2$  sensor [40]. A nanostructured conducting polymer could immobilize with glutamate micro bio-sensor has been proved amperometrically to be capable of showing their enhanced performance in *in vitro* sensor studies [41]. A simple electrostatic assembly method has been used for the fabrication of ultrathin sulfonated polyaniline (SPAN) with poly(diallyldimethylammonium) film exhibited higher electrocatalytic ( $\sim 3$  nm) reduction of  $\text{H}_2\text{O}_2$  [42].

#### 2.4. Composites

A  $\text{TiO}_2/\text{SiO}_2$  composite has been synthesized by sol-gel method and it quenched by the presence of phosphorescence (Wavelength = 403 nm), the electrode catalysts were exhibited better electrocatalytic activities towards to  $\text{H}_2\text{O}_2$  [43].

Wu *et al* [44] have proposed a novel new zinc porphyrin-fullerene ( $\text{C}_{60}$ ) derivative like a  $\text{ZnP-C}_{60}$  derivative of para- $\text{ZnP}_p\text{-C}_{60}$  and ortho- $\text{ZnP}_o\text{-C}_{60}$ . In this kind of fullerene based derivatives, which could entrap with tetraoctylammonium bromide (TOAB) on GCE. The modified electrode (TOAB/ $\text{ZnP}_p\text{-C}_{60}$ /GCE) catalysts were evaluated by both cyclic voltammetry (Fig.3A) and amperometric (Fig.3B) techniques using  $\text{H}_2\text{O}_2$  analyte. The composite exhibited four-well defined redox peaks and highly sensitive ( $215.6 \mu\text{A mM}^{-1}$ ) and lowest detection ( $0.81 \times 10^{-6}$  M) of  $\text{H}_2\text{O}_2$ . A mediatorless oxidase/peroxidase composite has been prepared by the sol-gel method. A general observation was made for the direct electron transfer from the electrode surface to horseradish peroxidase (HRP) and glucose [45]. For the first time, Xiao *et al* [46] ultrasonic electrochemically gold-platinum nanoparticles were deposited on Chitosan (Ch)-ionic liquid (Trihexyltetradecylphosphonium bis(trifluoromethane sulfonyl)imide,  $[\text{P}(\text{C}_6)_3\text{C}_{14}] [\text{Tf}_2\text{N}]$ ) film electrode for  $\text{H}_2\text{O}_2$  reduction ie, the LOD of  $\text{H}_2\text{O}_2$  was estimated to be 0.3 nM. Cyclic voltammetry and amperometry techniques were used as excellent electrocatalytic techniques for investing electrochemical behaviour of myoglobin based graphene oxide and nafion (Mb-GO-Nafion) composite. The activity myoglobin modified film electrode displayed remarkable electrocatalytic towards  $\text{H}_2\text{O}_2$  biosensor applications [47]. Xia *et al* [48] reported the important role that template-free electrode fabrication of metal-metal oxide based graphene ( $\text{Pt-MnO}_2/\text{graphene}$ ) nanohybrid composite in biosensor ( $\text{H}_2\text{O}_2$ ) for biomedical (liver cells) applications. A covalent immobilization of pyruvate oxidase (PyO) onto the poly-5,2':5',2''-terthiophene-3'-carboxylic acid (Poly-TTCA(Nano-CP))

electrode served as an excellent host matrix for amperometrically detection of the phosphate solution [49]. The combinations of platinum nanoparticles were deposited on CNT (CNT+Pt<sub>Nano</sub>) nanocomposite has shown to exhibit remarkable bio-catalytic detected (1.5 to 150  $\mu$ M) [50].

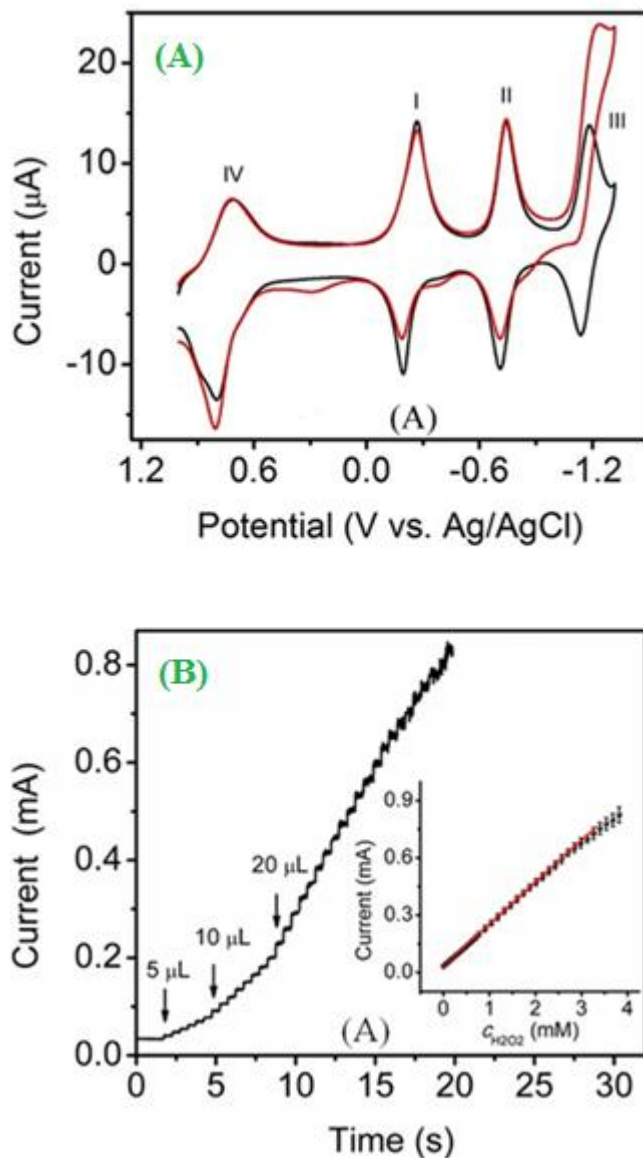


**Figure 3.** CVs of TOAB/ZnP<sub>p</sub>-C<sub>60</sub>/GCE in 0.5 M KCl aqueous solution (A) before and after the addition of 0.615 mM H<sub>2</sub>O<sub>2</sub>. (B) Representative amperometric current-time curves of TOAB/ZnP<sub>p</sub>-C<sub>60</sub>/GCE in 4.0 mL stirring 0.5 M KCl aqueous solution with successive additions of 0.028 M H<sub>2</sub>O<sub>2</sub>. ("Reprinted with permission from (*Anal. Chem.*, 86 (2014) 6285-6290). Copyright (2014) American Chemical Society").

### 3. VARIOUS SYNTHESIS METHODS

There are several methods of preparation of different kinds of electrode materials for the analysis of biosensors (H<sub>2</sub>O<sub>2</sub>, glucose oxidase and cholesterol oxidase) based systems. Sheet structures

of boron-doped graphene nanosheet materials that have prepared by a carbothermal method and it can be used for metal-free electrochemical estimation of enzyme based biosensor applications [51]. A simple and cost-effectiveness of hydrothermal method is a most promising technique, which can be used for the fabrication of silver nano particles (AgNPs) supported reduced graphene oxide (rGO) carbon nanotube (MWCNT) composite [52]. One of the green synthesis of chemical reduction method (At room temperature) widely used for the preparation of Cu<sub>2</sub>O nano cubes wrapped with graphene nano sheets (Cu<sub>2</sub>O/GNs) electrocatalyst in non-enzymatic electrochemical evaluations [53]. A facile hydrothermal (At 130° C) approach of low-cost and effective approach for preparing different CuO (Heart/dumbbell-like and grass-like) nanostructure electrodes. The two different nanostructured electrode materials were exhibited good electrochemical response in biosensor [54]. Particularly, the new type of paper-like structure of MnO<sub>2</sub> nano wire-graphene nano hybrid (MnO<sub>2</sub>-ERGO) electrode by one-step electrochemical method may increase the electrocatalytic activity of H<sub>2</sub>O<sub>2</sub> [55]. Enormous efforts have been made to synthesize (Sol-gel method) peroxide based graphite electrode act as a host matrix with the electroenzymatic system involves with the direct electron transfer from the electrode surface of HRP and graphite particles [56]. Fang *et al* [57] suggested self-assembled method, which can highly loaded AuNPs (11-18 nm) on 2D-graphene nano sheets (GN-AuNPs) heterostructures have been employed the enhanced electrochemical behaviour of H<sub>2</sub>O<sub>2</sub>. The porous structure of a gas diffusion electrode (GDE) serves as promising materials for investigating the *in situ* generation of H<sub>2</sub>O<sub>2</sub> in direct electrochemical reduction of oxygen by electrochemical flow-reactor [58].

## 4. MORPHOLOGICAL EFFECTS

### 4.1. Nanoparticles

Jiang *et al* [59] made silver nanoparticles (AgNPs) electrochemically deposited on the boron doped diamond electrode with hemoglobin.

This result showed a suitable nanoparticle modified electrode with dendritic and aggregated AgNPs were varied from 100 nm to 2 μm. The electrocatalytic properties have been carried out by both cyclic voltammetry and chronoamperometry techniques, the reported detection limit of 1.5 μM in CV and 4.3 μM in chronoamperometry, respectively. Maji *et al* [60] investigated the H<sub>2</sub>O<sub>2</sub> sensor on a new kind of two-dimensional immobilized gold nanoparticles (AuNPs, ~3 nm) on the sandwich-like periodic mesoporous silica (PMS) modified reduced graphene oxide (rGO), which was fabricated by chemical method. The HRTEM image (Fig.4A) of RGO-PMS@AuNPs selected area electron diffraction pattern. The displayed electrochemical performance of H<sub>2</sub>O<sub>2</sub> detection limit (60 nM) and excellent sensitivity (39.2 μA mM<sup>-1</sup> cm<sup>-2</sup>) from human urine (Fig.4B). On the other hand, the development of platinum (2.5 nm) based nanoparticles were deposited on graphite electrode for the study of H<sub>2</sub>O<sub>2</sub> activity and their sensitivity [61]. The usefulness of spherical Au nanoparticle modified with electro active Prussian blue (PB@Au) hybrid composite for the construction of the H<sub>2</sub>O<sub>2</sub> sensor [62]. The low-cost and small scale production of as-prepared electroactive based polyethyleneimine (PEI) supported rhodium nanoparticles (Rh-NPs) deposited on graphite screen-printed (SPEs)

electrode was immobilized with citrate anions and it detects for  $\text{H}_2\text{O}_2$  produced by auto oxidation of phenols from tea extract. The immobilization based Ru-NPs/SPEs electrode offer highly sensitive and good recovery (97 and 104 %) for chemical on-site sensor applications [63]. Campbell *et al* [64] discussed for the possible two-parallel cathodic  $\text{H}_2\text{O}_2$  reduction mechanisms (Normal and autocatalytic) by using silver nanoparticle array electrode in acidic conditions. In this modified AgNPs array size decreases, the negative peak shift also decreases, on the other hand the positive peak shift also increases for  $\text{H}_2\text{O}_2$  reduction.

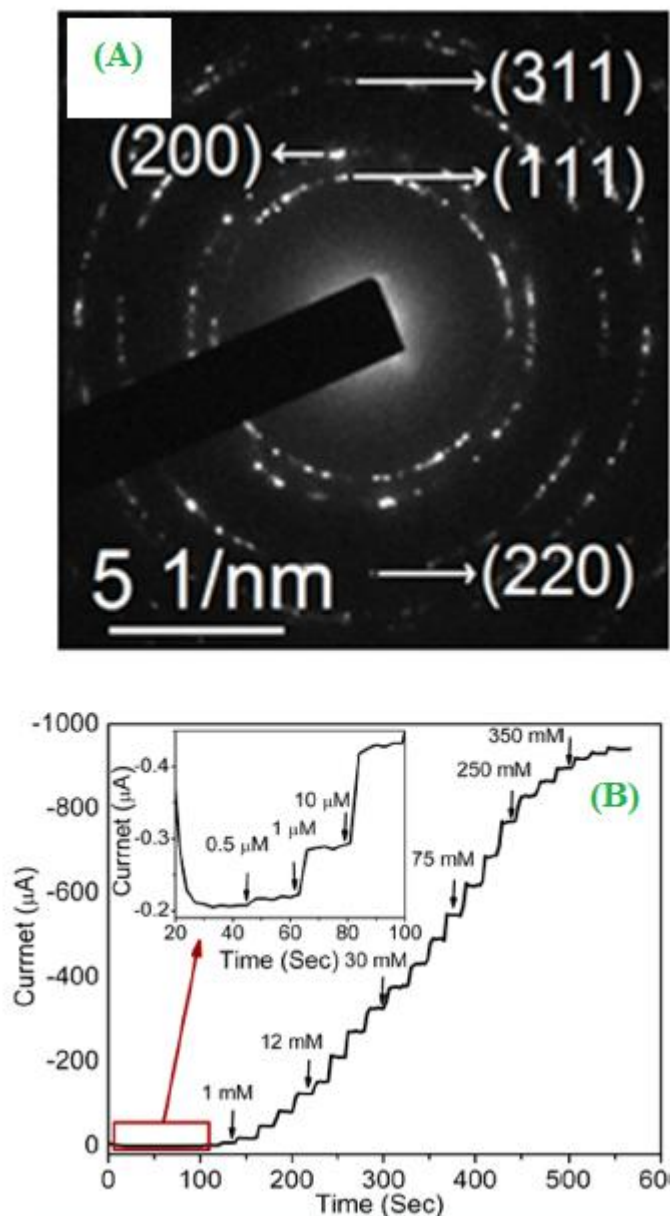


**Figure 4.** (A) HRTEM image of SAED pattern of RGO-PMS@AuNPs. (B) Amperometric response curve for RGO-PMS@AuNPs/GC electrode by the successive addition of  $\text{H}_2\text{O}_2$  into 0.1 M PBS at -0.75 V. ("Reprinted with permission from (*ACS Appl. Mater. Interfaces* 6 (2014) 13648-13656). Copyright (2014) American Chemical Society").

#### 4.2. Nano wire

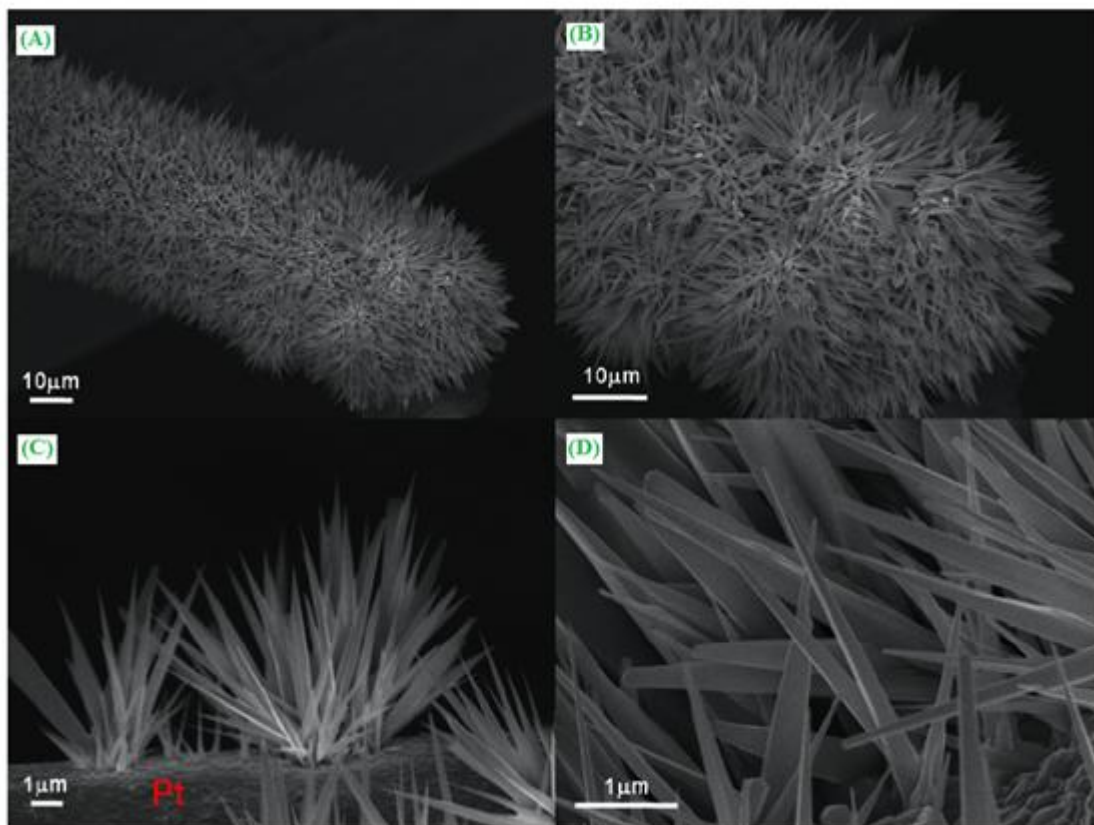


**Figure 5.** As grown  $\text{IrO}_2$  nanowires on a Pt microwire (diameter = 25  $\mu\text{m}$ ). (A-D) SEM images with different magnifications showing hierarchically grown  $\text{IrO}_2$  nanowires on a 25  $\mu\text{m}$  Pt microwire. ("Reprinted with permission from (*Anal. Chem.*, 84 (2012) 3827-3832) Copyright (2012) American Chemical Society").

A powerful strategy of surface growing method has been used for the fabrication of hierarchically crystalline based iridium dioxide ( $\text{IrO}_2$ ) nano wire in platinum (Pt) micro wire electrode. SEM images (Fig.5(A-D)) were clearly showing their electrode surface micro wire diameter around 25  $\mu\text{m}$  and the electrocatalytic activity of  $\text{IrO}_2$ -Pt composites has been further investigated for kinetically controlled reaction of both  $\text{H}_2\text{O}_2$  and NADH by amperometrically [65]. Zhao *et al* [66] reported the use of hyper branched  $\text{Cu@Cu}_2\text{O}$  co-axial nano wire mesh electrode remarkably enhanced the bio-sensing molecule sensitivity, response rate, stability and reproducibility.

#### 4.3. Quantum dots

Basically, nanomaterials are defined in the nature of dimensionalities such as quantum dots, quantum wire and quantum well *etc.* A simple surfactant free in situ growth of AuNPs of nitrogen-doped graphene quantum dots (AuNPs-N-GODs) electrode. The composites (AuNPs-N-GODs) have

been studied by X-ray photoelectron spectroscopy (XPS) (Fig.6A), which were observed three predominant peaks at 284.0 for C<sub>1s</sub>, 400.0 for N<sub>1s</sub> and 530.0 eV for O<sub>1s</sub>.

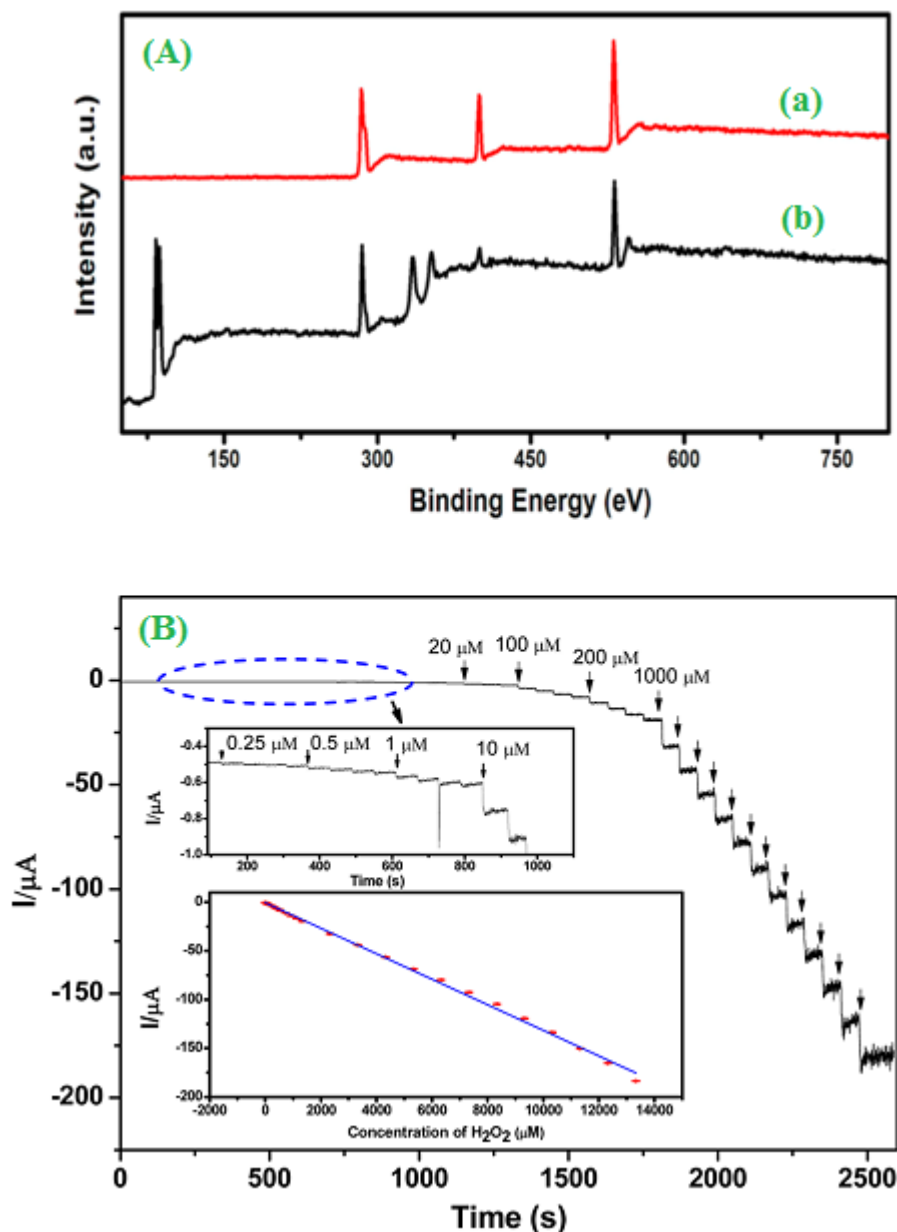


**Figure 6.** (A) XPS survey spectra of N-GQDs (line a) and Au NPs-N-GQDs (line b) (B) Amperometric responses of the Au-NPs/N-GQDs/GC electrode to the successive addition of H<sub>2</sub>O<sub>2</sub> (Applied potential: -0.3V). Insets show the magnified amperometric response to the low H<sub>2</sub>O<sub>2</sub> concentration (top) and the corresponding calibration plot for the Au NPs-N-GQDs/GC electrode. ("Reprinted with permission from (*Anal. Chem.* 87 (2015) 1903-1910) Copyright (2015) American Chemical Society").

In this matrix (AuNPs-N-GODs), average size increased to 5.2 nm and the electrocatalytic measurements were carried out by using amperometrically ie. The LOD of H<sub>2</sub>O<sub>2</sub> is  $0.12 \times 10^{-6}$  M (Fig.6.B) [67]. The performance of quantum based light-controllable gold modified CdS and FePt nano

particles monolayer has been evaluated by different  $\text{H}_2\text{O}_2$  concentrations. The immobilized quantum dot based layer electrode, which can influence the bio-sensing properties [68].

## 5. OPTIMIZATION PARAMETERS (pH)

Most of the biosensor molecules have been immobilized with the related compounds and its pH sensitive transistor for the electrode incorporated with enzyme and acetylcholine. One of the most interesting bio-specific interaction between lactim protein Concanavalin A (Con A) and glycoenzyme horseradish peroxidase (HRP) were deposited on pyrolytic graphite (PG) electrode. By using this HRP immobilized  $\{\text{Con A/HRP}\}_n$  film electrode could realize the pH controllable electrochemical reduction of  $\text{H}_2\text{O}_2$  and  $[\text{Fe}(\text{CN})_6]^{3-}$  was used as a mediated solution (Fig.7A).

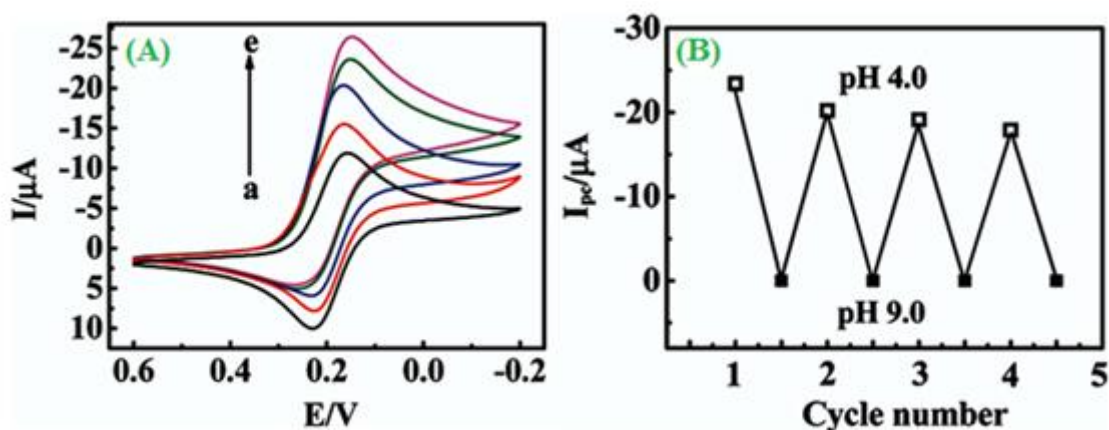


**Figure 7.** (A) CVs of  $\{\text{Con A/HRP}\}_5$  films at  $0.01 \text{ V s}^{-1}$  in pH 4.0 buffers containing  $1 \text{ mM K}_3\text{Fe}(\text{CN})_6$  and  $\text{H}_2\text{O}_2$  at (a) 0, (b) 0.06, (c) 0.14, (d) 0.18, and (e) 0.26 mM. (B) Dependence of the CV electrocatalytic reduction peak current ( $I_{pc}$ ) on solution pH switched between pH 4.0 (0) and 9.0 (9) for the same  $\{\text{Con A/HRP}\}_5$  films. ("Reprinted with permission from (*J. Phys. Chem. B* 114 (2010) 3380-3386) Copyright (2010) American Chemical Society").

This kind of study, which can be used for better understanding of the mechanism of pH sensitive and fabrication of pH controllable bio-electro catalysts with the immobilized enzyme based studies (Fig.7B) [69]. Hydrogen peroxide redox reaction (HPRR) is a typical example for the optimization of pH studies. Here, the initial potential studies of both oxygen reduction reaction (ORR) and HPRR exhibited the same and the observed polarization curves were optimized at  $\text{pH} = 4$ . In general, ORR exhibits  $4e^-$  series pathway, on the other hand, HPRR for the  $2e^-$ , respectively [70]. More specifically, a bio-compatibles of poly(N-isopropyl acrylamide)-g-poly(N-isopropyl acrylamide-Co-styrene) (PNIPAM-g-P(NIPAM-Co-St)) nanoparticles has been synthesized by the free emulsion polymerization method. In this nanoparticles were immobilized with hemoglobin (Hb) and it was mixed with MWCNTs (PNNS/MWCNTs/GCE) film electrode. The immobilized electrode has been optimized at various pH (Optimized pH range is 5.0 to 9.0) using cyclic voltammetry techniques. The

bioactive PNNS/MWCNTs film electrode was electro catalytically examined ( $\text{LOD} = 2.9 \times 10^{-8} \text{ M}$ ) to the reduction of  $\text{H}_2\text{O}_2$  [71]. To explore the electrochemical bio-sensors, great effort have been developed for the detection of  $\text{O}_2$ ,  $\text{H}_2\text{O}_2$  and pH related ions by using three different (Platinum black, Tungsten oxide ( $\text{W}/\text{WO}_3$ ) and iridium oxide ( $\text{Pt}/\text{IrO}_2$ )) ultra micro electrodes. By the above discussed electrodes, Pt black microelectrodes were displayed more sensitive and the pH optimized for the detection of  $\text{O}_2$  and  $\text{H}_2\text{O}_2$  [72]. The kinetic reactions were examined between tetrathionate and  $\text{H}_2\text{O}_2$ , the experimental observed mechanisms were accurately studied in alkaline conditions and it provides a new insight autocatalytic nature in  $\text{H}_2\text{O}_2$  and thiosulfate- $\text{Cu}^{2+}$  reaction [73].

## 6. ELECTROCHEMICAL SENSITIVE TECHNIQUES

### 6.1. Chronoamperometry

Notably, a facile and cost-effective well-defined silver dendrites (Branched dendrite diameter range 70-80 nm) Au modified nanostructures have attracted considerable attention and it has been widely used amperometric technique for  $\text{H}_2\text{O}_2$  detection [74]. A fundamental challenge in peptide based nano tube concerns the use of amperometric biosensors for the sensitive monitoring of glucose and  $\text{H}_2\text{O}_2$ . By this modified (Peptide-nano tube) electrode significantly  $\text{H}_2\text{O}_2$  current response up to 100 nA [75]. Polyvinylpyrrolidone stabilized palladium nano sphere electrode attracted great attention for their favourable electro analytical determination of  $\text{H}_2\text{O}_2$ . The optimized modified electrodes were exhibited versatile sensing performance in  $\text{H}_2\text{O}_2$  and their demonstrated LOD to 8 nM. The possible palladium based electrode, which can be used for interesting electro active species, such as ascorbic acid (AA), uric acid (UA) and acetaminophen (AP) [76]. One of the most notable  $\text{H}_2\text{O}_2$  biosensors have been optimized by the amperometric method by using polyelectrolyte (Citrate)-stabilized with gold electrode (CS-AuNPs). Having a good sensitive of CS-AuNPs enzymatically performed with the biosensor molecules [77]. Due to the bio-sensor applications, a biomediator electrode can be modified with graphite, thionine and nickel hexacyanoferrate (TH/NiHCF). TH/NiHCF electrode showed the current enhancement of electrocatalytic activity towards gallic acid (GA) and  $\text{H}_2\text{O}_2$  estimation from the commercially available (Green tea and milk) samples [78]. Electrocatalyst is one of the most popular research in biosensor applications, the conductive thionine and aminoalkane thionols were immobilized with few-walled carbon nanotubes (FWCNTs) for the important electrochemical properties. In this typical amperometric response of FWCNT/thionine/Au electrode reported the estimated  $\text{H}_2\text{O}_2$  LOD value of  $1.14 \times 10^{-6} \text{ M}$  [79]. Wang *et al* [80] have fabricated a three-dimensional nanoporous (NP) PtAu alloy electrode by simple and general de-alloying method. The authors were highly focused on highly sensitive and comparable electrode catalysts (Pt/C and NP/PtAu) for the superior sensing performance towards glucose and  $\text{H}_2\text{O}_2$ .

### 6.2. Differential pulse voltammetry

Differential pulse voltammetry (DPV) is a versatile technique for the analysis of both organic and inorganic compounds. And also, this technique may analyzed by the following important

parameters like sample period, pulse width and pulse amplitude. A core-shell nanostructure of Pt and gold supported polyethyleneimine functionalized carbon nanotubes (Pt@Au/PEI-MWCNTs/GCE) have been fabricated by seed-mediated growth method. Therefore, the modified functionalized nano composites were greatly improved for the electrocatalytic reduction of  $\text{H}_2\text{O}_2$  ( $3.1 \times 10^{-8}$  M) [81]. Another important application of platinum based polyaniline (PANI) was electrodeposited on meso porous silica film electrode (MSF), which it exhibited good electrocatalytic activity toward non-enzyme based bio-sensor applications [82]. A numerous DPV experimental observations were made of immobilized enzyme (Horseradish peroxidase) doped  $\text{SnO}_2$  (HRP/Nano-Ni- $\text{SnO}_2$ ) nanoparticle film, the nano (43 nM) detection of  $\text{H}_2\text{O}_2$  [83]. A novel uniformly distributed copper-doped copper oxide nano scale metal oxides (Average diameter  $\sim 50$  nm) have emerged as another important class of electrode materials for covering a broad range (0.005 - 8 mM) of electrochemical analysis in gaseous form of  $\text{H}_2\text{O}_2$  by DPV [84]. The use of cystamine (Cys) immobilized electroactive iron(III)diethylenetriamine Penta acetic acid (DTPA- $\text{Fe}^{\text{III}}$ ) complex was modified with nanoporous gold electrode (NPG). The yielded unique information for better understanding of the DTPA- $\text{Fe}^{\text{III}}$  and  $\text{H}_2\text{O}_2$  interaction, electron transfer reaction [85]. Silver nanoparticle (AgNPs) have been electro fabricated with ionic liquid functionalized multi-walled carbon nanotube (AgNPs/MWCNTs-IL) on GCE for the study of a novel nonenzymatic  $\text{H}_2\text{O}_2$  sensor applications, the notable catalytic LOD of  $3.9 \times 10^{-9}$  M and the exhibited linear response logarithm of the  $\text{H}_2\text{O}_2$  range from  $1.2 \times 10^{-8}$  to  $4.8 \times 10^{-6}$  M [86].

### 6.3. Square wave voltammetry

In this technique, this can be used as an alternative voltammetry method for the improvement of sensitivity of electroanalytical tool. The horseradish peroxidase based co-substrate  $\text{H}_2\text{O}_2$  find wide applications in biosensor based co-substrate samples, such as phenol, *o*-phenylenediamine, 3,3',5,5'-tetramethylbenzidine (TMB), hydroquinone, *p*-chlorophenol, pyrocatechol and *p*-aminophenol etc. From these SWV calibrated co-substrate systems, only *o*-phenylenediamine exhibited best substrate for HRP enzyme based reaction [87]. Gold deposited glassy carbon electrode (Au/GCE) has been reported to be examined for the simultaneous detection of per acetic acid (PAA) and  $\text{H}_2\text{O}_2$ . By this gold deposited electrode contained citric acid ( $\text{Au}_{\text{cit}}$ /GCE) displayed the highest electrocatalytic activity towards PAA and  $\text{H}_2\text{O}_2$  [88]. A picco molar detection of  $\text{H}_2\text{O}_2$  was studied at the chemically active redox mediator in buffer solutions (pH = 5.0). The remarkable reported LOD value about 8 pM and the Michaelis-Menten rate constant ( $k_m$ ) value was estimated from the immobilized HRP ( $84 \pm 13$  and  $504 \pm 19$   $\mu\text{M}$ ) [89].

## 7. SENSORS

### 7.1. Ascorbic acid

The widespread interest biological study of ascorbic acid (AA) interference study of  $\text{H}_2\text{O}_2$  behaviour using glucose oxidase immobilized poly(*o*-phenylenediamine) modified Pt (PPD/ $\text{GO}_x$ /Pt)

electrode. By this electrode was successfully made reduced the direct faradic interference electroactive species to an AA concentration level in glucose [90]. A non-oxidative approaches interference study of Au sputtered coating single-stranded DNA immobilized poly(aniline boronic acid) modified carbon nanotube (ssDNA/SWNT/PABA/Au) composite has been evaluated by fluorescence emission spectra (FES) for the sensitive detection of ascorbic acid (AA) (Fig.8) [91]. Different approaches have been made for disposable screen-printed electrode modification with *o*-aminophenol based electrode applied the detection of AA in fresh fruits, vegetables and commercial juices (LOD =  $0.86 \times 10^{-6}$  M) [92]. Among the biological studies, so far constructed a new strategy of ratio metric immobilized thionine/Ketjen black (KB) nanocomposite effectively assisted electrochemical sensor for *in vivo* detection of AA in living brain [93]. Bossi *et al* [94] used easily polymerizable polyaniline on a micro titer reader plate was easy for the testing of AA from real samples (Soft drinks and fruit juice) by iodometric method.

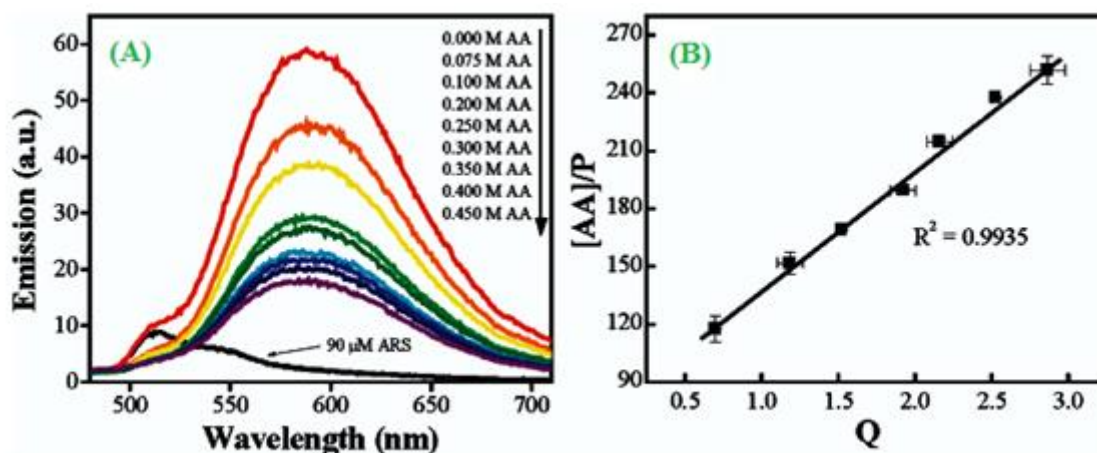
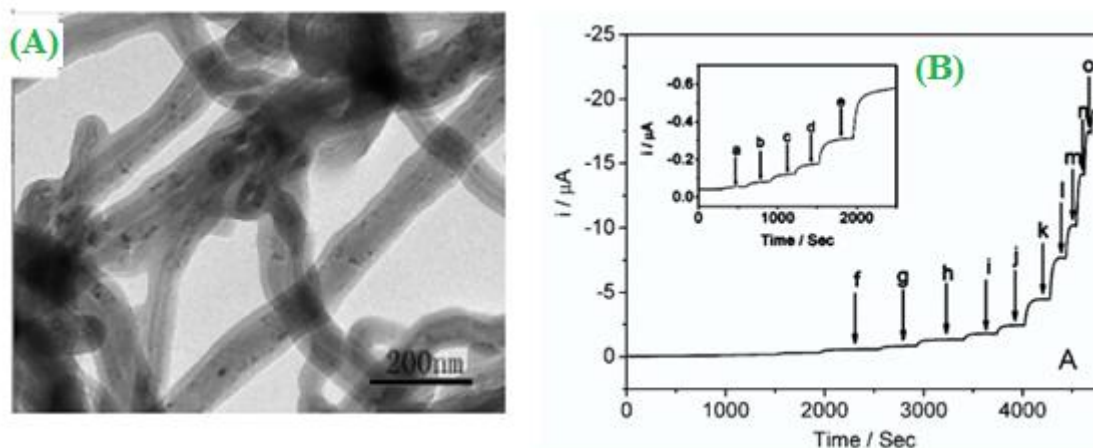


**Figure 8.** Fluorescent binding assay results of the affinity between PBA and AA and between PBA and DA: (A) fluorescence emission curves of the PBA-ARS complex upon titration with a range of AA concentrations; (B) linear correlation between  $[AA]/P$  and  $Q$  (see the Experimental Section for explanation). ("Reprinted with permission from (*J. Phys. Chem. B 111* (2007) 12275-12281) Copyright (2007) American Chemical Society").

Zhao *et al* [95] reported electrochemical deposition of H-terminated Si(100) substrate based spherical cobalt core-shell nanoparticle electrode. They also reported the feasibility of high performance bio-sensor for AA evaluation.

## 7.2. Dopamine

Khan *et al* [96] applied a novel multi-walled carbon nanotube and molecular imprinted polymer (MIP) (MWCNTs/MIP) composite for the simultaneous determination of highly sensitive and selective detection of dopamine (DA) and AA (Fig.1B).



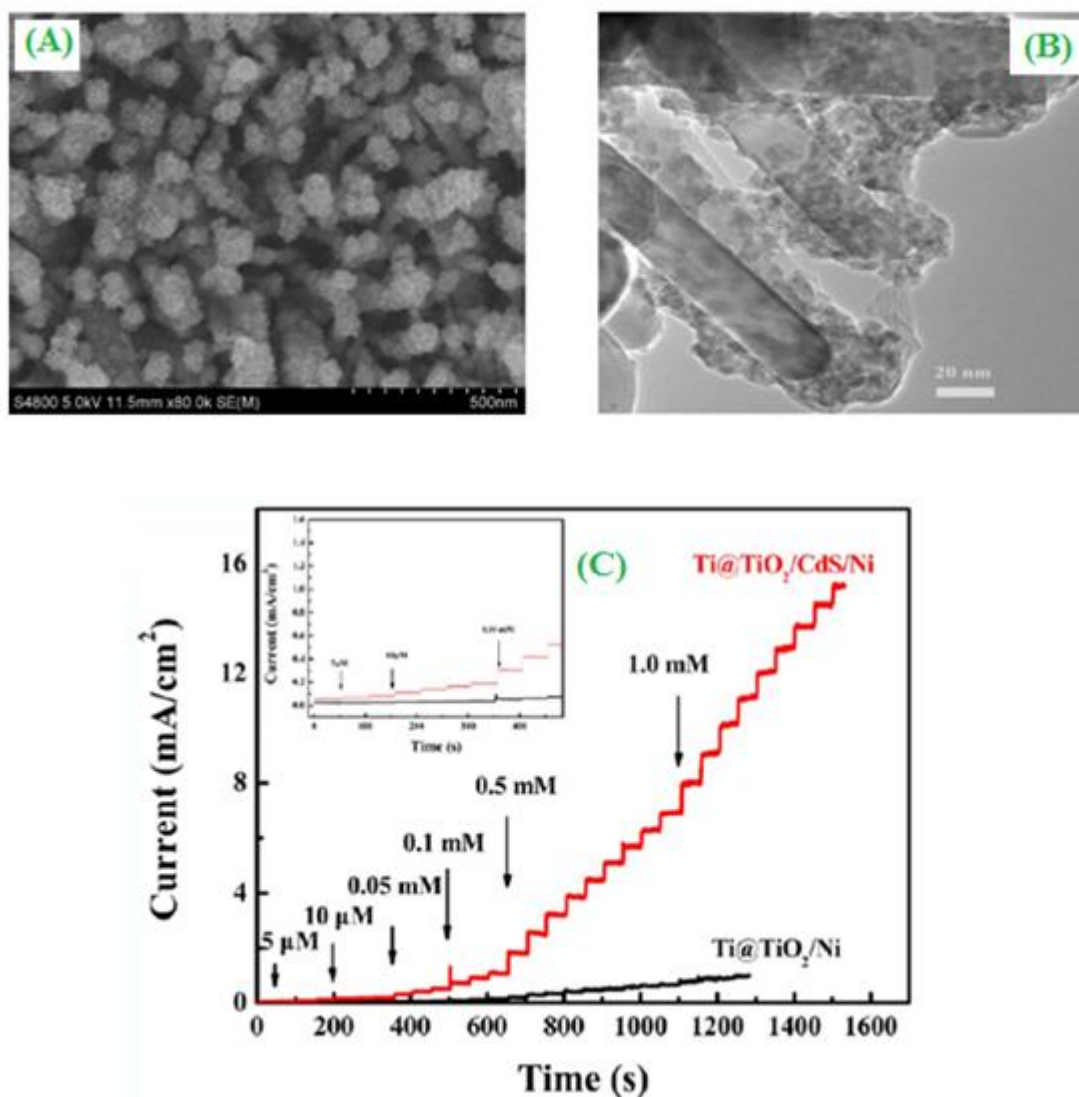
**Figure 9.** (A) TEM image of MWNTs-MIPs1. (B) Typical current response curve at MWNTs-MIPs1 modified glassy carbon electrode with addition of increasing concentration of DA in PBS. Applied potential: +0.3V and validation curve for DA obtained by  $I$ - $T$  curve. ("Reprinted with permission from (*J. Phys. Chem. C* 112 (2008) 4849-4854) Copyright (2008) American Chemical Society").

Fig.9A. Shows the TEM image morphological structure of MWCNTs/MIP, the estimated wall and length average thickness value 20 nm. The high performance of newly developed non-oxidative self-doped poly(aniline boronic acid) modified carbon nanotube (PABA/CNT) composites have the capability of high sensitive electrooxidation of dopamine and its potential application in Parkinson's diseases [97]. The electrochemical polymerization of polyacetyltriamine (PACty) modified with sulfobutyl ether- $\beta$ -cyclodextrin (SBCD) on boron-doped diamond (BDD) electrode displayed the noticeable amperometric responses of DA,  $\gamma$ -dihydroxy phenylnediamine (L-DOPA), epinephrine (EP) and norepinephrine (NEP) [98]. Recently, the dual stabilizer-capped CdSe and quantum dots (QDs) were covalently immobilized with *p*-amino benzoic acid on GCE. The proposed accurately quantifying dopamine sensor value ranges from 10.0 nM to 3.0  $\mu$ M from the real samples of drug, human urine and cerebro-spinal fluid *etc* [99]. A uniform and reproducible enzymatic (Glucose oxidase) nontronite based clay modified electrode was prepared on the GCE. The immobilized clay electrode reported the common interference studies of DA and glucose (LOD of DA =  $7.4 \times 10^{-6}$  M) [100]. Moreover, the self-assembled method has been used for the incorporation of corrole on Au electrode surface. Here, corrole act as an ion channel mimetic sensor for the good sensitivities toward DA (LOD of DA is  $10^{-12}$  M) [101].

### 7.3. Glucose

Yamazaki *et al* [102] constructed a new strategy and novel electrode catalyst of *Escherichia Coli* (*E-Coli*) based pyrroloquinone quinone glucose dehydrogenase (PQQGDH) and His-775 employed colorimetric analytical system for the determination of glucose concentration level over 60 times (0.5 - 30 mM). Besides, a highly oriented nicotinamide adenine dinucleotide-dependent-glucose dehydrogenase (NAD-GDH) has been synthesized by Paal-Knorr condensation method. It was further constructed with a new electron mediator in 5-[2,5-di(thiophene-2-yl)-1H-pyrrole-1-yl]-1,10-

phenanthroline iron (III) chloride (FePhenTPy) on a screen printed carbon electrode (SPCE) for the optimized analytical performance of the proposed glucose sensor with the LOD of  $12.02 \pm 0.6 \text{ mg dL}^{-1}$  [103]. Recently, a bi-functional (Ni/CdS) and core-shell ( $\text{Ti@TiO}_2$ ) nanowire electrode was successfully fabricated by both hydrothermal and electrodeposition methods.



**Figure 10.** (A) Top-view FESEM images of  $\text{Ti@TiO}_2/\text{CdS}/\text{Ni}$  sample (B) TEM images of  $\text{Ti@TiO}_2/\text{CdS}/\text{Ni}$ . (C) Amperometric response of  $\text{Ti@TiO}_2/\text{CdS}/\text{Ni}$  and  $\text{Ti@TiO}_2/\text{Ni}$  electrodes to successive additions of glucose at an applied potential of 0.55 V. Inset: a partial magnification of the current response toward a low concentration of glucose solution. ("Reprinted with permission from (*Anal. Chem.* 86 (2014) 876-883) Copyright (2014) American Chemical Society").

Fig.10.A. shows the top-view of the field emission scanning electron microscopy (FESEM) of  $\text{Ti@TiO}_2/\text{CdS}/\text{Ni}$  electrode. From the morphological, structural analysis, TEM image of  $\text{Ti@TiO}_2/\text{CdS}$  which indicated their average particle size up to 150 nm (Fig.10B). The extended study of amperometric glucose sensor of  $\text{Ti@TiO}_2/\text{CdS}$  achieved 95 % steady-state current (2s) and the

detection limit current value  $0.35 \times 10^{-6}$  M (Fig.C) [104]. Similarly, the different morphological (Nanocoral, branched belt, nanothorn and nanoparticle) electrode catalysts were widely used in low onset potential based selective glucose sensor by a simple electrochemical deposition method. Among these electrode catalysts, nanocoral electrode reported the highest anodic current response ( $1.0 \times 10^{-6}$  M) than others [105]. The supramolecular of *Aloe vera leaf*-like morphology based polyaniline supported copper(I) composite being electro active and it provides a high sensitivity, fast response and low level electrochemical detection of non-enzymatic glucose [106]. Zen *et al* [107] reported the enzymatic clay (Nontronite, *SWa-1*) modified electrode the normal cyclic voltammetric determination of glucose in 0.1M phosphate buffer solution (pH = 7) with  $5.0 \times 10^{-6}$  M as the possible limit of reproducible detection. The use of chronoamperometry technique, which was used for the electro-oxidation of glucose concentration reaches at  $4.8 \times 10^{-5}$  M by CuNi dendritic electrode [108]. In the electrochemical (Biosensors and supercapacitors) fields, Pongam seed shells-derived activated carbon and cobalt oxide (PSAC/Co<sub>3</sub>O<sub>4</sub>) nanocomposite material was one of the versatile electrodes that can be applied to the enzyme free glucose (21 nM) sensor and supercapacitor (Highest specific capacitance = 94 F g<sup>-1</sup>) applications [109].

#### 7.4. Uric acid

A novel attempt to be made for the successful construction of poly(N-methyl-*o*-phenylenediamine) (Poly-MPD) modified with gold (Au) electrode and it can further immobilize with uric acid oxidase (UO<sub>x</sub>). The use of redox ladder polymer (Poly-MPD/UO<sub>x</sub>/Au) composite for the determination of consumption rate of uric acid and the significant anodic current enhancement was obtained around  $0.066 \mu\text{A cm}^{-2}$  (30 s) by the amperometric method [110]. A three-dimensional (3D) network based graphene foam (GF) has been synthesized by chemical vapour deposition (CVD) on indium tin oxide (ITO) glass electrode. Uric acid was detected based on the simultaneous determination using ascorbic acid (AA). It was analytically quantitatively by differential pulse voltammetry (DPV) with a detection limit 3 nM [111]. Chen *et al* [112] prepared a fast response, broad linear and satisfactory stability, low potential detection bio-sensor of uricase-thionine-SWCNTs/GC (UO<sub>x</sub>-Th-SWCNTs/GC) composite greatly applicable for the determination of UA by cyclic voltammetry method (Fig.11A).

In this composite created a negative charge distribution occurred through hydrophobic interaction between sodium do-decyl benzene sulfonate (SDBS) and SWCNTs. The displayed fast response (2s) detection limit value of  $0.5 \pm 0.05 \times 10^{-6}$  M and high sensitivity ( $\sim 90 \mu\text{A mM}^{-1} \text{cm}^{-2}$ ) for good reproducibility (Fig.11B). To investigate the electrochemical deposition of poly(chromotrope 2B)-modified anodic glassy carbon electrode (PCHAGCE) under neutral (pH = 7) conditions. The fabricated electrode presented good capacity to accumulate UA and hence applied to its determination to the micro-molar concentration level ( $1.5 \pm 0.03 \times 10^{-6}$  M) [113]. The self-assembled biomimetic based L- $\alpha$ -phosphatidylcholine  $\beta$ -oleoyl- $\gamma$ -palmitoyl (PCOP) and bi-layer of n-octanethiolate (OT) on the Au electrode was extensively studied for the rapid amperometric determinations of UA and their  $K_M^{app}$  ( $1.32 \text{ mM d}^{-3}$ ) [114].

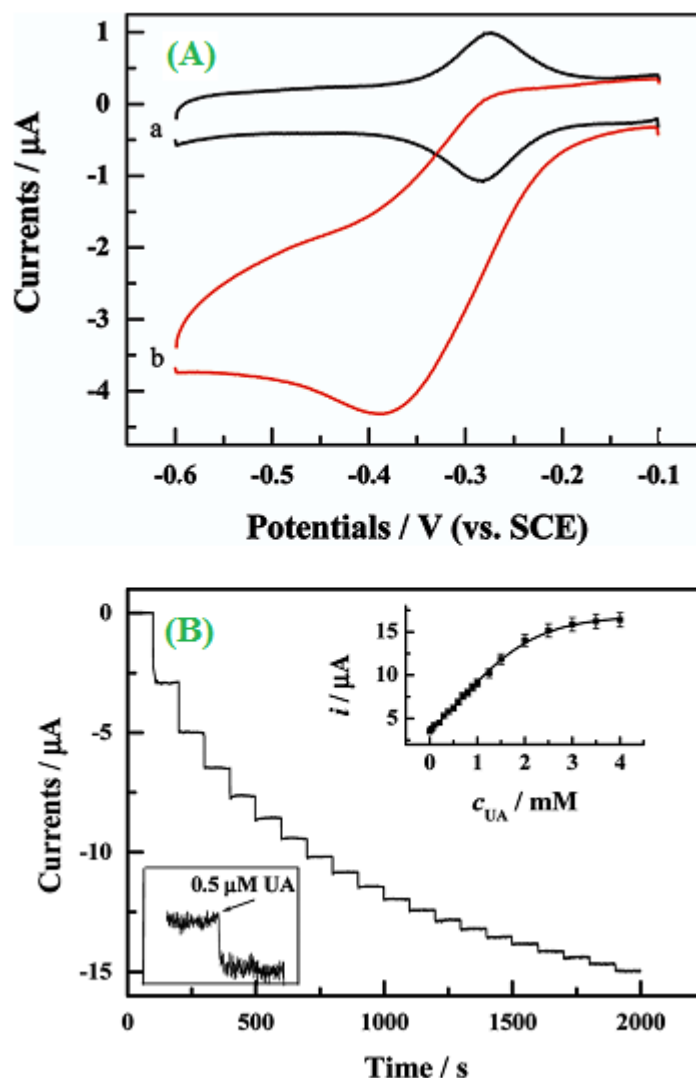


**Figure 11.** (A) Cyclic voltammograms of the  $\text{UO}_x\text{-Th-SWNT/GC}$  electrode in air-saturated PBS with (b) and without (a) 0.1 mM UA. The scan rate is  $5 \text{ mV s}^{-1}$ . (B) Amperometric responses of the  $\text{UO}_x\text{-Th-SWNT/GC}$  to the successive addition of UA in PBS (0.1 M, pH 7.4) at an applied potential of  $-400 \text{ mV}$ . Each addition of UA is  $50 \mu\text{M}$ . The inset shows the dependence of the response of the electrode on UA concentration under the optimal condition. ("Reprinted with permission from (*Anal. Chem.* 82 (2010) 2448-2455) Copyright (2010) American Chemical Society").

In another related study, the selective reusability growth of boron doped diamond (BDD) microelectrode importantly selective determination of UA in the presence of AA [115]. The performance of clay (Cameroonian smectite)/porphyrine (Chloromeso-tetraphenyl porphyrine iron (III)) based composite had been evaluated for the successful simultaneous determinations of AA, UA and nitrate ( $\text{NO}_2^-$ ) and their respective LOD values of 0.95, 0.06 and  $0.5 \times 10^{-6} \text{ M}$ , respectively [116]. Lavanya *et al* [117] have constructed a novel biosensor of  $\text{SnO}_2/\text{graphene}$  nanocomposite by a simple one-pot chemical reduction method, which was studying the synchronized determinations of EP and UA from the interference of AA.

## 8. ELECTRODE STABILITY

There have been few studies on the uses of a stable modified electrode in the development of nonenzymatic biosensor application of H<sub>2</sub>O<sub>2</sub>. You *et al* [118] fabricated a stable, flat and uniform Pt nanoparticle embedded graphite-like carbon matrix (Pt-NEGCF) proved to be a suitable detected traced level bio molecule of H<sub>2</sub>O<sub>2</sub>. Another H<sub>2</sub>O<sub>2</sub> sensor was developed based on unique combination properties of mesoporous (HI-ePt) microelectrode reported the outstanding qualitative and quantitative amperometric sensor for the detection ( $4.5 \times 10^{-6}$  M) of H<sub>2</sub>O<sub>2</sub> [119]. A novel phthalocyanine based metalated (M(Cu, Co and Ni)-Pc) and metal-free (H2-Pc) chemiresistive electrodes were fabricated for the sensing of H<sub>2</sub>O<sub>2</sub>. This kind of new approach offered selectively identify for the presence of H<sub>2</sub>O<sub>2</sub> [120]. Recently, Sheng *et al* [121] suggested the direct electrochemistry of electroactive hemoglobin immobilized fullerene based nitrogen-doped carbon nanotube and Chitosan (C<sub>60</sub>-NCNTs/CHIT) composite was obtained excellent electrocatalytic ability towards the H<sub>2</sub>O<sub>2</sub> reduction. Fe<sub>3</sub>O<sub>4</sub>/PPy/Ag nanocomposite based on core/shell/shell structure was developed for the detection of H<sub>2</sub>O<sub>2</sub>. The electrochemical signal of the biosensor reaction was observed at -0.2 V. Using chronoamperometry, the limit of detection for H<sub>2</sub>O<sub>2</sub> was found to be  $1.7 \times 10^{-6}$  M [122]. Goncalves [123] have also developed a novel nonenzymatic H<sub>2</sub>O<sub>2</sub> sensor based on poly(3,4-ethylenediamine thiophene)/poly(neutral red) electrode, which exhibited a remarkable catalytic performance for the detection of H<sub>2</sub>O<sub>2</sub> ( $80 \times 10^{-6}$  M dm<sup>-3</sup>). The significant development of an accurate and low-cost nickel foam based *Cytochrome c* (Cyt.c/Ni foam) modified electrode has been monitoring the electrochemical detection of H<sub>2</sub>O<sub>2</sub>. By this modification of Ni foams and Cyt.c could enhance their electrocatalytic, sensitivity, selectivity and detection limit of H<sub>2</sub>O<sub>2</sub> ( $2 \times 10^{-7}$  M) [124]. Azizi *et al* [125] developed an inexpensive and environmentally friendly mesoporous silica based SBA-16 nanoparticle modified with stem cane ash (SCA) on Ag (Ag/SBA-16/CPE) electrode was fabricated by the sol-gel method. This composite was reported to be highly efficient to capture H<sub>2</sub>O<sub>2</sub> facilitating the enrichment of H<sub>2</sub>O<sub>2</sub> on to its surface. Moreover, an innovative of Prussian-blue modified carbon nanotube based paste electrode for the best performance of H<sub>2</sub>O<sub>2</sub> and it exhibited good repeatability, reproducibility and electrochemical stability up to 500 cycles [126].

## 9. CONCLUSIONS

In summary, we have discussed novel kinds of electrode materials, and their nonenzymatic biosensor applications. In specifically, the authors were highlighted different electrode materials and their electrochemical sensor behaviors were analyzed by the electro analytical (Chronoamperometry, DPV and SWV) techniques. The successful construction of a new type of biosensor electrode catalysts one of the most promising alternative biological applications, because they could report good electrocatalytic activity and high sensitivity towards the oxidation of H<sub>2</sub>O<sub>2</sub>. Finally, the prospects and future challenges of novel based modified nanocomposites for high performance in sensitive, selective and reproducible for the biosensor detection of H<sub>2</sub>O<sub>2</sub>.

## ACKNOWLEDGEMENT

We gratefully acknowledged, The Management and Chemistry Department Staff members, The Madura College, Madurai, Tamil Nadu, India. And also we thankful to Mr. Abhijit Manna, JRF, SBS, DAB & P, MKU, for his valuable discussion in this article.

## References

1. M. Elkaoutit, I.N. Rodriguez, M. Dominguez, M.P.H. Artiga, D.B. Milla, J.L.H.D. Cisneros, *Electrochim. Acta* 53 (2008) 7131-7137.
2. A. Salimi, M. Mahdoui, A. Noorbakhsh, A. Abdolmaleki, R. Ghavami, *Electrochim. Acta* 56 (2011) 3387-3394.
3. Y. Xin, X.F. Bing, L.H. Wei, W. Feng, C.D. Zhao, W.Z. Yang, *Electrochim. Acta* 109 (2013) 750-755.
4. Y. Han, J. Zheng, S. Dong, *Electrochim. Acta* 90 (2013) 35-43.
5. Y. Li, F. Huang, Z. Luo, B. Xu, X. Wang, F. Li, F. Wang, L. Huang, S. Li, Y. Li, *Electrochim. Acta* 74 (2012) 280-286.
6. Y. Zhang, Z. Chu, L. Shi, W. Jin, *Electrochim. Acta* 56 (2011) 8163-8167.
7. D. Ye, H. Li, G. Liang, J. Luo, X. Zhang, S. Zhang, *Electrochim. Acta* 109 (2013) 195-200.
8. L.G. Macia, M.R. Smyth, A. Morrin, A.J. Killard, *Electrochim. Acta* 58 (2011) 562-570.
9. Y. Zheng, Y. Liu, J. He, P. Pang, Y. Gao, Q. Hu, *Electrochim. Acta* 90 (2013) 550-555.
10. C. Sun, W. Li, Y. Sun, X. Zhang, J. Shen, *Electrochim. Acta* 44 (1999) 3401-3407.
11. Q. Sheng, H. Yu, J. Zheng, *Electrochim. Acta* 52 (2007) 7300-7306.
12. X. Au, F. Teng, P. Zhang, C. Zhao, X. Pan, Z. Zhang, E. Xie, *J. Alloys Compd.*, 614 (2014) 373-378.
13. R. Villalonga, P. Diez, P.Y. Seden, J.M. Pingarron, *Electrochim. Acta* 56 (2011) 4672-4677.
14. J.S. Easow, T. Selvaraju, *Electrochim. Acta* 112 (2013) 648-654.
15. S.M. Chen, R. Ramachandran, V. Mani, R. Saraswathi *Int. J Electrochem. Sci.*, 9 (2014) 4072-4085.
16. R. Ramachandran, V. Mani, S.M. Chen, G. Gnana kumar, P. Gajendran, N.B. Devi, R. Devasenathipathy *Int. J Electrochem. Sci.*, 10 (2015) 3301-3318.
17. K.J. Babu, A. Zahoor, K.S. Nahm, R. Ramachandran, M.A.J. Rajan, G. Gnana kumar, *J. Nanopart. Res.* 16 (2014) 2250.
18. R. Ramachandran, V. Mani, S.M. Chen, G. Gnana kumar, M. Govindasamy *Int. J. Electrochem. Sci.*, 10 (2015) 859-869.
19. R. Ramachandran, V. Mani, S.M. Chen, R. Saraswathi, B.S. Lou, *Int. J Electrochem. Sci.*, 8 (2014) 11680.
20. R. Ramachandran, S.M. Chen, G.P. Gnana kumar, P. Gajendran, N.B. Devi, *Int. J Electrochem. Sci.*, 10 (2015) 8607-8629.
21. R. Ramachandran, S.M. Chen, G.P. Gnana kumar, *Int. J Electrochem. Sci.*, 10 (2015) 8581-8606.
22. R. Ramachandran, S.M. Chen, G.P. Gnana kumar, *Int. J Electrochem. Sci.*, 10 (2015) 7111-7137.
23. Y. Xu, P.E. Pehrsson, L. Chen, R. Zhang, W. Zhao, *J. Phys. Chem. C* 111 (2007) 8638-8643.
24. X. Jia, G. Hu, F. Nitze, H.R. Barzergar, T. Sharifi, C.W. Tai, T. Wagberg, *ACS. Appl. Mater. Interfaces* 5 (2013) 12017-12022.
25. X. Xu, S. Jiang, Z. Hu, S. Liu, *ACS Nano* 4 (2010) 4292-4298.
26. A.S. Kumar, P. Gayathri, P. Barathi, R. Vijayaraghavan, *J. Phys. Chem. C* 116 (2012) 23692-23703.
27. S. Dong, N. Li, G. Suo, T. Huang, *Anal. Chem.*, 85 (2013) 11739-11746.
28. C. Song, P.E. Pehrsson, W. Zhao, *J. Phys. Chem. B* 109 (2005) 21634-21639.

29. M.Y. Hua, H.C. Chen, R.Y. Tsai, S.J. Tseng, S.C. Hu, C.D. Chiang, P.J. Chang, *J. Phys. Chem. C* 115 (2011) 15182-15190.
30. Y. Li, B. Tan, Y. Wu, *J. Am. Chem. Soc.*, 128 (2006) 14258-14259.
31. W. Liu, H. Zhang, B. Yang, Z. Li, L. Lei, X. Zhang, *J. Electroanal. Chem.*, 749 (2015) 62-67.
32. M. Roushani, E. Karami, A. Salimi, R. Sahraei, *Electrochim. Acta* 113 (2013) 134-140.
33. N. Butwong, L. Zhou, W.N. Eonate, R. Burakham, E. Moore, S. Srijaranai, J.H.T. Luong, J.D. Glennon, *J. Electroanal. Chem.*, 717 (2014) 41-46.
34. J. Kivrak, O. Alal, D. Atbas, *Electrochim. Acta* 176 (2015) 497-503.
35. C. Cheng, Y. Huang, N. Wang, T. Jiang, S. Hu, B. Zhang, H. Yuan, D. Xiao, *ACS Appl. Mater. Interfaces* 7 (2015) 9526-9533.
36. C. Qi, J. Zheng, *J. Electroanal. Chem.*, 747 (2015) 53-58.
37. H. Yoon, S. Ko, J. Jang, *J. Phys. Chem. B* 112 (2008) 9992-9997.
38. D. Raffa, K.T. Leung, F. Battaglini, *Anal. Chem.*, 75 (2003) 4983-4987.
39. T. Hoshi, H. Saiki, S. Kuwazawa, C. Tsuchiya, Q. Chen, J.O.I. Anzai, *Anal. Chem.*, 73 (2001) 5310-5315.
40. E.S. Forzani, H. Zhang, L.A. Nagahara, I. Amlani, R. Tsui, N. Tao, *Nano. Lett.*, 4 (2004) 1785-1788.
41. M.A. Rahman, N.H. Kwon, M.S. Won, E.S. Choe, Y.B. Shim, *Anal. Chem.*, 77 (2005) 4854-4860.
42. X. Yu, G.A. Sotzing, F. Papadimitrakopoulos, J.F. Rusling, *Anal. Chem.*, 75 (2003) 4565-4571.
43. X. Shu, Y. Chen, H. Yan, S. Gao, D. Xiao, *Anal. Chem.*, 79 (2007) 3695-3702.
44. H. Wu, S. Fan, X. Jin, H. Zhang, H. Chen, Z. Dai, X. Zou, *Anal. Chem.*, 86 (2014) 6285-6290.
45. L.C. Guerente, S. Cosnier, P. Labbe, *Chem. Mater.*, 9 (1997) 1348-1352.
46. F. Xiao, F. Zhao, Y. Zhang, G. Guo, B. Zeng, *J. Phys. Chem. C* 113 (2009) 849-855.
47. C. Guo, H. Sun, X.S. Zhao, *Sens. Actuators, B* 164 (2012) 82-89.
48. F. Xiao, Y. Li, X. Zan, K. Liao, R. Xu, H. Duan, *Adv. Funct. Mater* 22 (2012) 2487-2494.
49. M.A. Rahman, D.S. Park, S.C. Chang, C.J.M. Neil, Y.B. Shim, *Biosens. Bioelectron.*, 21 (2006) 1116-1124.
50. S. Hrapovic, Y. Liu, K.B. Male, J.H.T. Luong, *Anal. Chem.*, 76 (2004) 1083-1088.
51. M.H. Yeh, Y.S. Li, G.L. Chen, L.Y. Lin, T.J. Li, H.M. Chuang, C.Y. Hsieh, S.C. Lo, W.H. Chiang, K.C. Ho, *Electrochim. Acta* 172 (2015) 52-60.
52. F. Lorestani, Z. Shahnava, P. Mn, Y. Alias, N.S.A. Manan, *Sens. Actuators, B* 208 (2015) 389-398.
53. M. Liu, R. Liu, W. Chen, *Biosens. Bioelectron.*, 45 (2013) 206-212.
54. P. Gao, D. Liu, *Sens. Actuators, B* 208 (2015) 346-354.
55. S. Dong, J. Xi, Y. Wu, H. Liu, C. Fu, H. Liu, F. Xiao, *Analytica. Chim. Acta* 853 (2015) 200-206.
56. L.C. Guerente, S. Cosnier, P. Labbe, *Chem. Mater.*, 9 (1997) 1348-1352.
57. Y. Feng, S. Guo, C. Zhu, Y. Zhai, E. Wang, *Langmuir* 26 (2010) 11277-11282.
58. R.M. Reis, A.A.G.F. Beati, R.S. Rocha, M.H.M.J. Assumpcao, M.C. Santos, R. Bertazzoci, M.R.V. Lanza, *Ind. Eng. Chem. Res.*, 51 (2012) 649-654.
59. L. Jiang, J. Hu, J.S. Food, *Electrochim. Acta* 176 (2015) 488-496.
60. S. Maji, S. Sreejith, A.K. Mandal, X. Ma, Y. Zhao, *ACS Appl. Mater. Interfaces* 6 (2014) 13648-13656.
61. T. You, O. Niwa, M. Tomita, S. Hirono, *Anal. Chem.*, 75 (2003) 2080-2085.
62. J.D. Qiu, H.Z. Peng, R.P. Liang, J. Li, X.H. Xia, *Langmuir*, 23 (2007) 2133-2137.
63. V.A. Gatselou, D.L. Giokas, A.G. Vlessidis, M.I. Prodromidis, *Talanta* 134 (2015) 482-487.
64. F.W. Campbell, S.R. Belding, R. Baron, L. Xiao, R.G. Compton, *J. Phys. Chem. C* 113 (2009) 9053-9062.

65. J.H. Shim, Y. Lee, K. Kang, J. Lee, J.M. Baik, Y. Lee, C. Lee, M.H. Kim, *Anal. Chem.*, **84** (2012) 3827-3832.
66. Y. Zhao, L. Fan, Y. Zhang, H. Zhao, X. Li, Y. Li, L. Wen, Z. Yan, Z. Huo, *ACS Appl. Mater. Interfaces* **7** (2015) 16802-16812.
67. J. Ju, W. Chen, *Anal. Chem.*, **87** (2015) 1903-1910.
68. W. Khalid, M.E. Helou, T. Murbock, Z. Yue, J.M. Montenegro, K. Schubert, G. Gobel, F. Lisdat, G. Witte, W.J. Parak, *ACS Nano* **5** (2011) 9870-9876.
69. H. Yao, N. Hu, *J. Phys. Chem. B* **114** (2010) 3380-3386.
70. S. Strbac, *Electrochim. Acta* **56** (2011) 1597-1604.
71. G. Zhang, N. Yang, Y. Ni, J. Sheng, W. Zhao, X. Huang, *Sens. Actuators, B* **158** (2011) 130-137.
72. A. Tsopela, A. Lale, E. Vanhove, O. Reynes, I. Seguy, P.T. Boyer, P. Juneau, R. Izquierdo, J. Launay, *Biosens. Bioelectron.*, **61** (2014) 290-297.
73. M. Voslar, P. Matejka, I. Schreiber, *Inorg. Chem.*, **45** (2006) 2824-2834.
74. X. Qin, Z. Miao, Y. Fang, D. Zhang, J. Ma, L. Zhang, Q. Chen, X. Shao, *Langmuir* **28** (2012) 5218-5226.
75. M. Yemini, M. Reches, E. Gazit, J. Rishpon, *Anal. Chem.*, **77** (2005) 5155-5159.
76. J. Sophia, Muralidharan, *J. Electroanal. Chem.*, **739** (2015) 115-121.
77. A.R. Schmidt, N.D.T. Nguyen, M.C. Leopold, *Langmuir* **29** (2013) 4574-4583.
78. N.S. Sangeetha, S.S. Narayanan, *Analytica. Chim. Acta* **828** (2014) 34-45.
79. M. Ma, Z. Miao, D. Zhang, X. Du, Y. Zhang, C. Zhang, J. Lin, Q. Chen, *Biosens. Bioelectron.*, **64** (2015) 477-484.
80. J. Wang, H. Gao, F. Sun, C. Xu, *Sens. Actuators, B* **191** (2014) 612-618.
81. W.W. Wei, Q. Yu, Z.S. Peng, L.J. Wei, L.X. Quan, L.X. Hui, *Chin J Anal Chem.*, **42** (2014) 835-841.
82. L. Ding, B. Su, *J. Electroanal. Chem.*, **736** (2015) 83-87.
83. N. Lavanya, S. Radhakrishnan, C. Sekar, *Biosens. Bioelectron.*, **36** (2012) 41-47.
84. H. Song, Y. Ni, S. Kokot, *Colloid and Surface A; Phisicochem. Eng. Aspects* **465** (2015) 153-158.
85. P. Li, Y. Ding, Z. Lu, Y. Chen, Y. Zhou, Y. Tang, C. Cai, T. Lu, *Analytica. Chim. Acta* **786** (2013) 34-38.
86. X. Li, Y. Liu, L. Zheng, M. Dong, Z. Xue, X. Lu, X. Liu, *Electrochim. Acta* **113** (2013) 170-175.
87. S.V. Kergaravat, M.I. Pividori, S.R. Hernandez, *Talanta* **88** (2012) 468-476.
88. M.I. Awad, T. Ohsaka, *Sens. Actuators, B* **221** (2015) 1335-1341.
89. J. L. Lyon, K.J. Stevenson, *Anal. Chem.*, **78** (2006) 8518-8525.
90. J.P. Lowry, R.D.O. Neill, *Anal. Chem.*, **64** (1992) 456-459.
91. S.R. Ali, R.R. Parajuli, Y. Ma, Y. Blogun, H. He, *J. Phys. Chem. B* **111** (2007) 12275-12281.
92. L. Cavit, H.M. Nassef, A. Fragoso, C.K.O. Sullivan, *J. Agri. Food. Chem.*, **56** (2008) 10452-10455.
93. H. Cheng, X. Wang, H. Wei, *Anal. Chem.*, **87** (2015) 8889-8895.
94. A. Bossi, S.A. Piletsky, E.V. Piletska, P.G. Righetti, A.P.F. Turner, *Anal. Chem.*, **72** (2000) 4296-4300.
95. L. Zhao, K. Liao, M. Pynenburg, L. Wong, N. Heinig, J.P. Thomas, K.T. Leung, *ACS Appl. Mater. Interfaces* **5** (2013) 2410-2416.
96. X. Kan, Y. Zhao, Z. Geng, Z. Wang, J.J. Zhu, *J. Phys. Chem. C* **112** (2008) 4849-4854.
97. S.R. Ali, Y. Ma, R.R. Parajuli, Y. Balogun, W.Y.C. Lai, H. He, *Anal. Chem.*, **79** (2007) 2583-2587.
98. F. Shang, L. Zhou, K.A. Mohmoud, S. Hrapovic, Y. Liu, H.A. Moynihan, J.D. Glennon, J.H.T. Luong, *Anal. Chem.*, **81** (2009) 4089-4098.
99. S. Liu, X. Zhang, Y. Yu, G. Zou, *Anal. Chem.*, **86** (2014) 2784-2788.
100. J.M. Zen, C.W. Lo, P.J. Chen, *Anal. Chem.*, **69** (1997) 1669-1673.

101. K. Kurzatowska, E. Dolusic, W. Dehaen, K.S. Stottny, A. Sieron, H. Radicka, *Anal. Chem.*, **81** (2009) 7397-7405.
102. T. Yamazaki, K. Kojima, K. Sode, *Anal. Chem.*, **72** (2000) 4689-4693.
103. D.M. Kim, M.Y. Kim, S.S. Reddy, J. Cho, C.H. Cho, S. Jung, Y.B. Shim, *Anal. Chem.*, **85** (2013) 11643-11649.
104. C. Guo, H. Huo, X. Han, C. Xu, H. Li, *Anal. Chem.*, **86** (2014) 876-883.
105. T.M. Cheng, T.K. Huang, H.K. Lin, S.P. Tung, Y.L. Chen, C.Y. Lee, H.T. Chiu, *ACS Appl. Mater. Interfaces* **2** (2010) 2773-2780.
106. M. Choudhary, S.K. Shukla, A. Taher, S. Siwal, K. Mallick, *ACS Sustainable Chem. Eng.*, **2** (2014) 2852-2858.
107. J.M. Zen, C.W. Lo, *Anal. Chem.*, **68** (1996) 2635-2640.
108. R. Qiu, X.L. Zhang, R. Qiao, Y. Li, Y.I. Kim, Y.S. Kang, *Chem. Mater.*, **19** (2007) 4174-4180.
109. R. Madhu, V. Veeramani, S.M. Chen, A. Manikandan, A.Y. Lo, Y.L. Chueh, *ACS Appl. Mater. Interfaces* **7** (2015) 15812-15820.
110. T. Nakaminami, S.I. Ito, S. Kuwabata, H. Yoneyama, *Anal. Chem.*, **71** (1999) 1928-1934.
111. H.Y. Yue, H. Zhang, J. Chang, X. Gao, S. Huang, L.H. Yao, X.Y. Lin, E.J. Guo, *Anal. Biochem.*, **488** (2015) 22-27.
112. D. Chen, Q. Wang, J. Jin, P. Wu, H. Wang, S. Yu, H. Zhang, C. Cai, *Anal. Chem.*, **82** (2010) 2448-2455.
113. X.B. Li, M.M. Rahman, G.R. Xu, J.J. Lee, *Electrochim. Acta* **173** (2015) 440-447.
114. T. Nakaminami, S.I. Ito, S. Kuwatata, H. Yoneyama, *Anal. Chem.*, **71** (1999) 4278-4283.
115. R. Kiran, E. Scorsone, P. Mailley, P. Bergonzo, *Anal. Chem.*, **84** (2012) 10207-10213.
116. J.C.K. Mbougouen, L. Angnes, *Sens. Actuators, B* **212** (2015) 464-471.
117. N. Lavanya, E. Fazio, F. Neri, A. Bonavita, S.G. Leonardi, G. Neri, C. Sekar, *Sens. Actuators, B* **221** (2015) 1412-1422.
118. T. You, O. Niwa, M. Tomita, S. Hirono, *Anal. Chem.*, **75** (2003) 2080-2085.
119. S.A.G. Evans, J.M. Elliott, L.M. Andrews, P.N. Bartlett, P.J. Doyle, G. Denault, *Anal. Chem.*, **74** (2002) 1322-1326.
120. F.I. Bohrer, C.N. Colesniuc, J. Park, I.K. Schullerr, A.C. Kummel, W.C. Trogler, *J. Am. Chem. Soc.*, **130** (2008) 3712-3713.
121. Q. Sheng, R. Liu, J. Zheng, *Bioelectrochemistry* **94** (2013) 39-46.
122. C. Qi, J. Zheng, *J. Electroanal. Chem.*, **747** (2015) 53-58.
123. A.R. Goncalves, M.E. Ghica, C.M.A. Brett, *Electrochim. Acta* **56** (2011) 3685-3692.
124. N. Akhtar, S.A.E. Safty, M. Khairy, W.A.E. Said, *Sens. Actuators, B* **207** (2015) 158-166.
125. S.N. Azizi, S. Ghasemi, A.S. Maybodi, M.R. Azad, *Sens. Actuators, B* **216** (2015) 271-278.
126. S. Husmann, E. Nossol, A.J.G. Zarbin, *Sens. Actuators, B* **192** (2014) 782-790.